# THE ACOUSTIC EXCITATION OF NEWLY-FORMED BUBBLES

GRANT DEANE, HELEN CZERSKI, DALE STOKES

Scripps Institution of Oceanography, UCSD
Code 0238, La Jolla, CA 92093-0238, USA
gdeane@ucsd.edu

*Gas bubbles in water act as oscillators with a natural frequency inversely proportional to their radius and a quality factor determined by thermal, radiation, and viscous losses. Newly-formed gas bubbles are excited into breathing mode oscillations immediately after creation, causing them to radiate a pulse of sound. Although the linear dynamics of spherical gas bubbles are well-understood, the mechanism driving the sound production has not been unambiguously identified. Using bubbles released from a nozzle as a model system, it can be shown that sound production is consistant with the rapid change in volume associated with the collapse of an air neck formed immediately after bubble pinch-off. The model is able to adequately describe the production of sound by bubbles released from a nozzle, and can also explain some of the acoustic properties of bubbles fragmenting in fluid turbulence. Laboratory experiments and model calculations of the mechanism are presented. [Work supported by ONR and NSF].*

## INTRODUCTION

The musical tones of running water are a familiar part of everyday life and are instantly recognizable. It has been known since the early part of the last century that these sounds are associated with the creation of bubbles, which behave like natural oscillators and produce a short pulse of sound at the moment of their formation[1]. Because of their importance to a wide range of subject areas, including medicine, chemical engineering, limnology, and oceanography, the behavior of spherical gas and cavitation bubbles has been well-studied[2]. The acoustic behavior of spherical gas bubbles is governed by the Rayleigh-Plesset equation, the validity of which has been verified by numerous theoretical and laboratory studies.

Despite the extensive body of literature on the acoustical properties of bubbles, little is known about the mechanism driving the production of sound when the bubble is first formed. Various mechanisms have been proposed[3], including the increase in external pressure

associated with a decrease in radius and accompanying Laplace pressure increase, hydrostatic pressure effects, non-linear, second order shape mode to volume mode coupling, and a fluid jet associated with the collapsing bubble neck. Estimates of the Laplace and hydrostatic pressure effects show that they probably make a minor (<10 %) contribution to the non-equilibrium initial conditions that excite acoustic radiation[3]. Shape mode to volume mode coupling may play an important role in the damping of highly distorted bubbles released from a nozzle or fragmenting[4], but a secondary role in bubble acoustic excitation.

Motivated by a desire to understand the underwater noise radiated by breaking waves, which is at least in part driven by the noise of bubbles fragmenting in fluid turbulence[5], we have studied the acoustic excitation of bubbles released from a nozzle. Nozzle-released bubbles represent a simple model system for the study of the non-equilibrium initial conditions driving acoustic emission.

## 1. BUBBLES RELEASED FROM A NOZZLE

Both small-scale laboratory and large-scale tank experiments were conducted to study the acoustic excitation mechanism of bubbles released from a nozzle. The small-scale laboratory measurements provided high-resolution photographs of the initial conditions immediately preceding bubble fragmentation while the tank measurements provided acoustic measurements relatively uncontaminated by reverberation.

For the laboratory measurements, a bubble-release nozzle was positioned 5cm above the base of a transparent acrylic tank with a 13 cm square cross-section. The tank was filled with either fresh or salt water to a depth of 25 cm. Air bubbles of approximately 2.2 mm radius were released at a nominal rate of 10 per minute. Bubble release was determined by interruption of a laser beam directed through the neck region, which was used to trigger photographic data acquisition and flash lighting. Flashes from two strobe lights, each of 15 μs duration, illuminated the bubble with a pre-programmed interval. Both images were superposed on a single frame, permitting observation of the neck development over short time intervals relative to the moment of neck rupture. The neck displacements were measured by increasing the inter-flash interval, with the first flash simultaneous with neck rupture. The neck velocity was measured using a short inter-flash interval with flash pairs occurring at successively later times after neck rupture.

The tank measurements were made on a frame deployed in a 15 m deep equipment test pool. A bubble injector consisting of a differential pressure regulator that provided a constant 60 kPa pressure above ambient fed a bubble injection nozzle via a constant gas flow valve. Bubbles were injected at a rate of approximately 30 per minute and acoustic signals were recorded with an International Transducer Corporation 6050C hydrophone mounted approximately 25 cm from the injection nozzle. The bubble injection system was positioned 2 m below the surface of the pool.

The geometry of a bubble immediately prior to release from the nozzle is illustrated in Figure 1. The bubble can be divided into three regions: a spherical region comprising the main volume of the bubble, a cylindrical region connecting the bubble to its parent volume (in this case, the air inside the nozzle) and a cone joining the cylindrical region to the spherical region. The cylindrical region is small compared with the overall bubble scale (0.3mm length versus 4.4 mm diameter) but the cone occupies a significant fraction of the overall bubble volume.

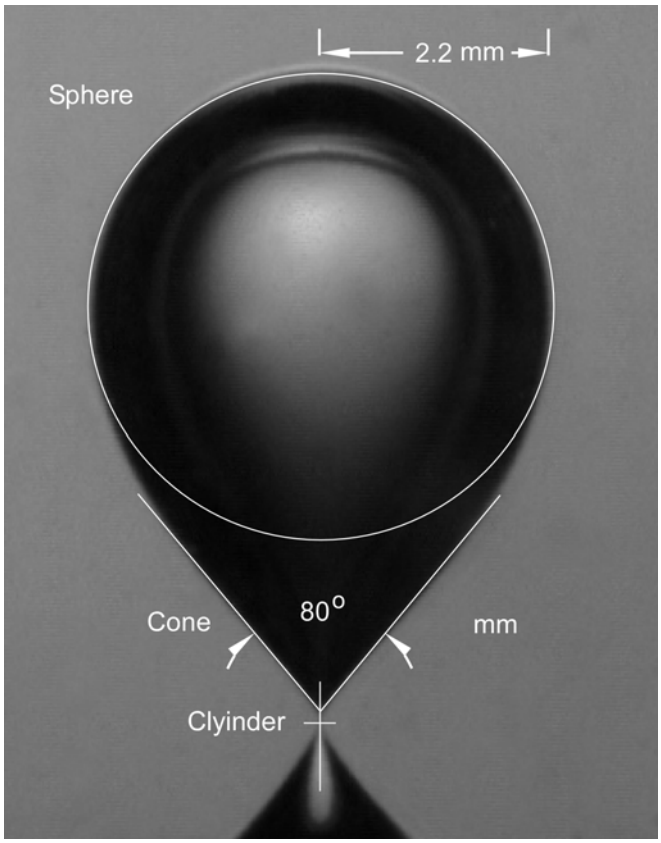


Fig.1 The geometry of a bubble released from the laboratory experiment nozzle. The cylindrical region is very narrow immediately prior to fragmentation and cannot be readily seen in the photograph

Detachment of the bubble from its parent volume occurs in the middle of the hyperbolic region and is accompanied by a very small radius of curvature at the two ends of the ruptured neck. The small radius of curvature is associated with a large Laplace pressure jump across the neck boundary, which accelerates the neck end away from the detachment point. The retraction of the conical neck remnant into the bubble initiates a rapid decrease in the bubble volume and drives the bubble into breathing mode oscillation.

A simple model for the neck retraction can formulated as follows. The conical section of the bubble is divided into a series of stacked disks. We assume that each disk is driven into motion by the conversion of surface tension energy at the boundary of the disk into kinetic energy through the disk volume. Beginning this calculation at the detachment point and integrating along the main bubble axis to a distance $x$ yields an expression for the neck velocity:

$$u = \begin{cases} \left(\dfrac{4\sigma}{\rho r_0}\right)^{1/2}, & x < x_0 \\ \left(\dfrac{4\sigma(1+\eta)^{1/2}}{\rho\eta x}\right)^{1/2}, & x \geq x_0 \end{cases} \tag{1}$$

where $x_0$ and $r_0$ respectively are the length and radius of the cylindrical region, $\sigma$ is the water surface tension (taken to be 0.072 N/m), $\rho$ is the water density and $\eta \approx 0.84$ is the

slope of the conical region. The time taken for the neck to collapse to a specified distance $x$ is found by integrating the reciprocal velocity and is given by:

$$\tau = \begin{cases} \left(\dfrac{\rho r_0}{4\sigma}\right)^{1/2} x, \; x < x_0 \\ \left(\dfrac{\rho r_0}{4\sigma}\right)^{1/2} x_0 + \dfrac{2}{3\eta}\left(\dfrac{\rho}{4\sigma(1+\eta^2)^{1/2}}\right)^{1/2} \left[(r_0 + \eta(x - x_0))^{3/2} - r_0^{3/2}\right], \; x \geq x_0 \end{cases} . \tag{2}$$

The neck collapse velocity and collapse time as a function of distance along the main bubble axis are plotted in Figure 2. This figure also includes measurements of these quantities made by analyzing photographs of the collapsing neck. Given the very simple nature of the neck collapse model, the agreement between the calculations and observation is encouraging. The neck collapse velocity is in error at most by a factor of 2 and reproduces the overall tend in collapse velocity reasonable well. The time versus distance curve is in reasonable agreement with the data until approximately 0.8 mm from the detachment point. Because the neck collapse model does not include any dissipation or deceleration mechanisms, such as fluid viscosity, capillary wave generation, and coupling between the neck and the bubble, it tends underpredicts the time required for the neck to collaspe at later times.

The rapid retraction of the detached neck into the bubble drives the bubble into breathing mode oscillation. The magnitude of the oscillation can be calculated by computing the decrease in neck volume with time and associating it with an overall decrease in bubble radius. The decrease in bubble radius is associated with an increase in gas pressure within the bubble, which can be calculated assuming a polytropic relation between gas pressure and volume. To carry the calculation further, we assume that the bubble is spherical and its motion is governed by the linearized Rayleigh-Plesset equation.

Although there is no direct way to accommodate the effects of the retracting neck into the Rayleigh-Plesset equation, we can compute the forcing function required to drive the required decrease in bubble volume by invoking continuity of normal stress across the bubble wall and neglecting surface tension and viscous forces there. The final result is a driving term on the right hand side of the Rayleigh-Plesset equation:

$$\frac{\partial^2 \varepsilon}{\partial t^2} + \left[\frac{4(\mu + \mu_{th})}{\rho R_0^2} + \frac{kR_0}{1 + k^2 R_0^2}\omega\right]\frac{\partial \varepsilon}{\partial t} + \left[\frac{3\kappa p_{in,0}}{\rho R_0^2} - \frac{2\sigma}{\rho R_0^3} + \frac{k^2 R_0^2}{1 + k^2 R_0^2}\omega^2\right]\varepsilon = f(t) \tag{3}$$

where ε is the fractional increase in bubble radius, μ is the fluid viscosity, $\mu_{th}$ is an effective thermal viscosity[6], $k$ and ω respectively are the wave number and angular frequency of sound at the bubble's natural frequency, $R_0$ is the bubble equilibrium radius, $p_{in,0}$ is the internal, equilibrium gas pressure inside the bubble, and the forcing function is given by:

$$f(t) = -\frac{9\kappa\sigma\eta\, p_{in,0}(1+\eta^2)^{1/2}}{4\rho^2 R_0^5} t^2; \;\; t > 0 . \tag{4}$$

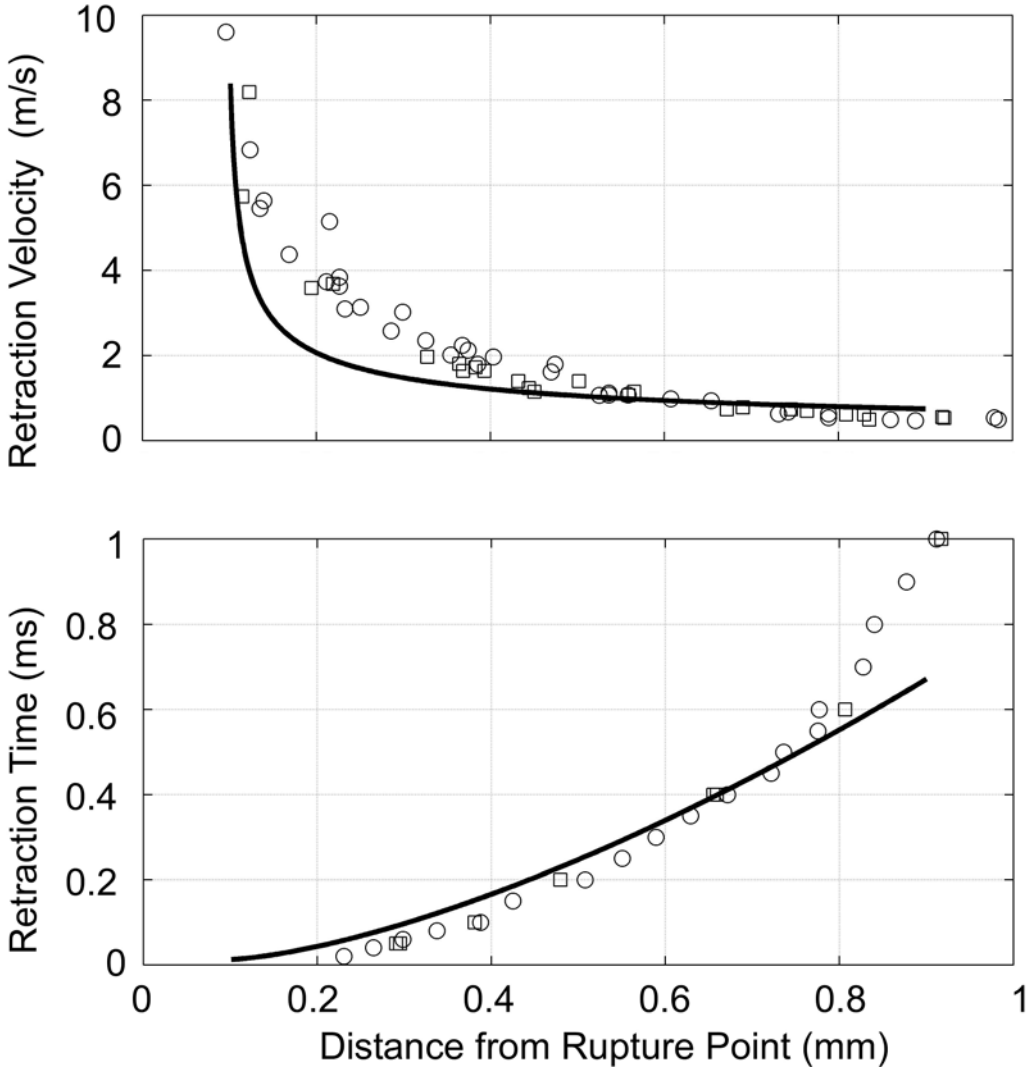


Fig.2 Comparison of the neck collapse model with experimental data. Circles and squares respectively correspond to fresh and salt water measurements. The cylinder radius (4.5 microns) was determined from the neck velocity at the end of the cylinder collapse and the cylinder length (100 microns) was estimated from the bubble photographs. The top plot shows the velocity of the collapsing neck as a function of distance from the detachment point. The bottom plot shows the collapse time as a function of distance from the detachment point

The effect of incorporating the forcing function described by Eq. (4) into the linearized Rayleigh-Plesset equation can be calculated by solving Eq. (3) using Runge-Kutta numerical integration. The result of this procedure is shown in Figure 3. The bottom plot shows the acoustic pressure measured at 1 m from the bubble center in the large tank experiment (solid black line) along with the pressure determined by numerical integration of Eq. (3) (broken black line). The dash-dot black line and gray lines are explained below. The top plot in Figure

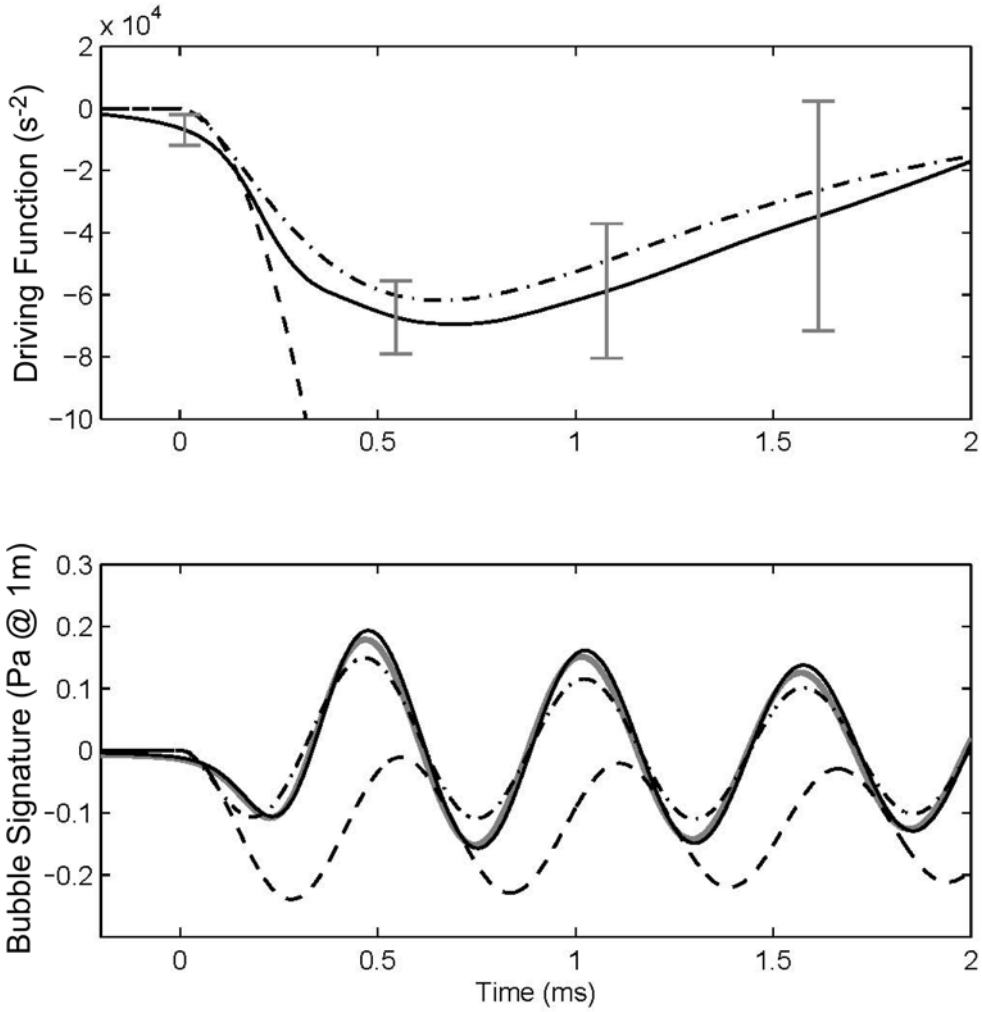


Fig.3 Top plot: Observed and modeled forcing functions plotted as a function of time. The solid, black line is the average of 50 forcing functions obtained from analysis of the acoustic pulse radiated by bubbles released from a nozzle. The four vertical, gray lines show the standard deviation in the estimate of the forcing function. The broken black line shows the theoretical forcing function based on the analytical model for neck collapse. The dash-dot black line shows the theoretical forcing function that includes an ad hoc modification for the effects of dissipation. Bottom plot: Observed and modeled pressure pulses. The solid black line shows the pressure pulse for a selected, average bubble. The solid grey, broken black and dash-dot lines respectively show calculated pulses for the observed, theoretical, and modified theoretical forcing functions

3 shows an analysis of the forcing function. The broken black line is the forcing function according to the neck collapse function described by Eq. (4). Without any damping mechanisms, it shows a quadratic increase over time without limit. The solid black line shows the forcing function determined by analyzing the acoustic radiation measured from the bubble. This is done by computing the bubble wall acceleration from the measured acoustic pressure, integrating the wall acceleration to obtain the wall velocity, and then integrating again to obtain the wall displacement. These three terms can then be added according to Eq. (3) to determine the forcing function required to produce the observed pressure field. The vertical gray lines show the standard deviation of the forcing function, determined by averaging 50

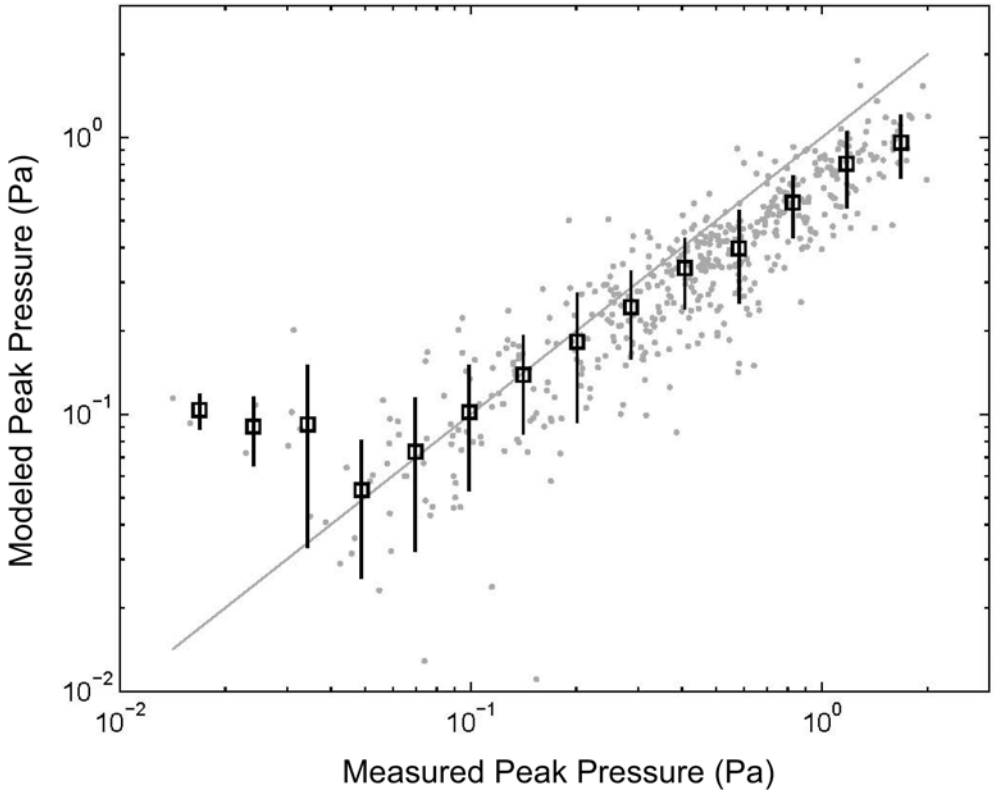


Fig.4 The predicted peak pressure versus observed pressure of the smaller bubble in a fragmentation product pair. The grey dots show a scatter plot of predicted versus observed pressure. The 14 black squares show the mean of the predicted peak pressure for all the data points lying within a bin centered on the square. The vertical black lines running through the center of the squares show the standard deviation of the data points. The solid grey line shows a 1:1 correspondence between predicted and observed pressures

observations. The dash-dot forcing line in the top plot shows an empirical forcing function based on the ideal quadratic form that includes the effects of damping on neck retraction. This function was constructed by introducing the time-varying exponent:

$$f(t) = -\frac{9\kappa\sigma\eta\, p_{in,0}(1+\eta^2)^{1/2}}{4\rho^2 R_0^5} t^{n(t)}; \quad t > 0 \tag{5}$$

where

$$n(t) = 469.5t + 1.955. \tag{6}$$

## 2. FRAGMENTING BUBBLES

The acoustic excitation model described in chapter 1 can be applied to fragmenting bubbles. Measurements of the sounds radiated by fragmenting bubbles were obtained by introducing bubbles between two opposing fluid jets placed directly above the injection nozzle. The resulting sound signatures were analyzed for peak pressure, frequency and decay rate as reported in Deane and Stokes[7]. The excitation model for fragmenting bubbles begins with the retracting neck model and adds the assumption that the neck of air joining the two

proto-bubbles immediately before fragmentation is symmetrical about the rupture point. The neck slope can be determined from the peak pressure radiated by one bubble product and used to predict the peak pressure of the other bubble product. The result of this analysis is shown in Figure 4, which shows predicted peak pressure versus observed peak pressure as grey dots. The black boxes show the mean predicted pressure for 14 amplitude bins. The vertical lines running through the boxes indicate the standard deviation of the data within an amplitude bin. The solid grey line shows a 1:1 correspondence between the observed and predicted pressures. Although there is significant scatter in the data, the mean predicted pressure follows the observed pressure well between 0.05 and 0.3 Pa. There is a systematic under-prediction of approximately 20% beginning at about 0.3 Pa and increasing to 100% at 2 Pa. The few data points at amplitudes less than 0.05 Pa do not show a good agreement between predicted and observed pressure.

## 3. CONCLUDING REMARKS

The sound produced by a bubble released from a nozzle is consistent with the forcing accompanying the collapse of the neck of air formed immediately after bubble detachment. The neck collapse is driven by surface tension forces and drives the bubble into oscillation by rapidly decreasing the bubble volume. An extension of the model to the sound radiated by fragmenting bubbles shows reasonable agreement with experiment.

## REFERENCES


1.M. Minnaert, On Musical Air Bubbles and the Sounds of Running Water, Philos. Mag., Vol. 16, 235-248 1933.

2.T.G. Leighton, The Acoustic Bubble, Academic Press, London 1994.

3.H.C. Pumphrey & J.E. Ffowcs Williams, Bubbles as Sources of Ambient Noise, IEEE J. Ocean Eng., Vol. 15, 268-274, 1990.

4.M.S. Longuet-Higgins, Nonlinear damping of bubble oscillations by resonant interaction, J. Acoust. Soc. Am., Vol. 91, 1414-1422, 1992.

5.G.B. Deane & M.D. Stokes, Scale dependence of bubble creation mechanisms in breaking waves, Nature, Vol. 418, 839-844, 2002.

6.A. Prosperetti, Thermal effects and damping mechanisms in the forced radial oscillations of gas bubbles in liquids, J. Acoust. Soc. Am., Vol. 61, 17-27, 1977.

7.G.B. Deane & M.D. Stokes, The acoustic signature of bubbles fragmenting in sheared flow, JASA-EL, Vol. 120, EL84-EL89, 2006.